© 2018. Published by The Company of Biologists Ltd | Journal of Experimental Biology (2018) 221, jeb185967. doi:10.1242/jeb.185967

RESEARCH ARTICLE

Convective oxygen transport during development in embryos of the snapping turtle *Chelydra serpentina*

Marina R. Sartori[1,2,*], Zachary F. Kohl[2], Edwin W. Taylor[1,3], Augusto S. Abe[1] and Dane A. Crossley, II[2]

ABSTRACT

This study investigated the maturation of convective oxygen transport in embryos of the snapping turtle (*Chelydra serpentina*). Measurements included: mass, oxygen consumption ($\dot{V}_{O_2}$), heart rate, blood oxygen content and affinity and blood flow distribution at 50%, 70% and 90% of the incubation period. Body mass increased exponentially, paralleled by increased cardiac mass and metabolic rate. Heart rate was constant from 50% to 70% incubation but was significantly reduced at 90% incubation. Hematocrit and hemoglobin concentration were constant at the three points of development studied but arteriovenous difference doubled from 50% to 90% incubation. Oxygen affinity was lower for the early 50% incubation group (stage 19) compared with all other age groups. Blood flow was directed predominantly to the embryo but was highest to the chorioallantoic membrane (CAM) at 70% incubation and was directed away from the yolk as it was depleted at 90% incubation. The findings indicate that the plateau or reduction in egg $\dot{V}_{O_2}$ characteristic of the late incubation period of turtle embryos may be related to an overall reduction in mass-specific $\dot{V}_{O_2}$ that is correlated with decreasing relative heart mass and plateaued CAM blood flow. Importantly, if the blood properties remain unchanged prior to hatching, as they did during the incubation period studied in the current investigation, this could account for the pattern of $\dot{V}_{O_2}$ previously reported for embryonic snapping turtles prior to hatching.

KEY WORDS: Cardiovascular, Blood oxygen content, Cardiac output, Hemoglobin affinity, Reptile, Microsphere distribution

INTRODUCTION

For developing animals, the cardiovascular system is an essential component of the oxygen cascade that supports metabolic rate. A number of key variables allow an organism to regulate this system to meet tissue oxygen demands during development. These include changing cardiac output and blood oxygen content (Tazawa and Mochizuki, 1977; Burggren et al., 2011). The role of the embryonic chorioallantoic membrane (CAM), the primary gas exchange surface (Piiper et al., 1980; Corona and Warburton, 2000), has been studied. However, the ontogeny of key parameters such as stroke volume of the heart, blood oxygen content and selective organ perfusion of most egg-laying vertebrates is poorly understood. Quantification of these and other components of convective oxygen transport is necessary to understand how embryos of egg-laying species, such as reptiles, adjust oxygen delivery as they progress through development.

Egg oxygen consumption increases with development as the mass of embryonic tissues increases due to growth and differentiation (Thompson, 1989; Booth, 1998a,b; Booth et al., 2000; Crossley et al., 2017a) and the convective oxygen transport system must be sufficient to supply this demand. While the components of oxygen delivery have not been extensively investigated in developing animals, metabolic rate has been studied in numerous species representing all reptilian lineages (Lynn and Von Brand, 1945; Dmi'el, 1970; Ackerman, 1981; Thompson, 1989; Booth and Thompson, 1991; Whitehead and Seymour, 1990; Thompson, 1993; Aulie and Kanui, 1995; Birchard and Reiber, 1995; Thompson and Stewart, 1997; Booth, 1998a,b; Vleck and Hoyt, 1991; Thompson and Russell, 1998, 1999; Booth et al., 2000; Sartori et al., 2017; Crossley et al., 2017a). The patterns of whole-egg metabolism in many species are characterized as peaking at some point prior to hatching followed by either a plateau or a decrease (Gettinger et al., 1984; Thompson, 1989; Miller and Packard, 1992; Booth, 1998a,b; Booth et al., 2000; Crossley et al., 2017a). The constant or dropping rate of oxygen consumption during the final period of incubation has been speculated to represent a period of time allowing for catch-up growth and simultaneous hatching in many reptilian species (Spencer et al., 2001). However, this pattern may merely represent a transition in the functional properties of convective transport.

In embryonic reptiles, direct measurements of stroke volume and blood oxygen content have not been conducted; however, heart rate and heart mass have been used to estimate cardiac output (Birchard and Reiber, 1996; Crossley and Altimiras, 2005; Nechaeva et al., 2007; Crossley et al., 2017a). Heart mass has been used as a proxy for stroke volume but this approximation has never been validated. Further, when attempting to characterize potential oxygen delivery to tissues using estimates of cardiac output, it is assumed that oxygen content and hemoglobin affinity are constant during development, which may not be the case. In common snapping turtles (*Chelydra serpentina*), embryonic heart rate drops approximately 20% between 70% and 90% incubation, a change that could result in an overall reduction in cardiac output (Eme et al., 2012; Alvine et al., 2013). Using heart mass as a proxy for stroke volume, a previous study of embryonic snapping turtles reported that cardiac output does not increase in proportion to embryonic mass, which would constrain metabolic function (Birchard and Reiber, 1996). This developmental window corresponds to a relative reduction or plateau in metabolic rate in snapping turtles, which may be attributed to a reduced convective transport ability (Crossley and Burggren, 2009). However, changes in blood properties could offset the apparent limit imposed by the cardiovascular system. These could comprise increased hematocrit and hemoglobin content,

[1]Departamento de Zoologia, Instituto de Biociências, Universidade Estadual Paulista, Campus Rio Claro, 13506-900 Rio Claro, SP, Brazil. [2]Department of Biological Sciences, Developmental Integrative Biology Cluster, University of North Texas, Denton, TX 76203-5017, USA. [3]School of Biosciences, University of Birmingham, Edgbaston B15 2TT, UK.

*Author for correspondence (marinarsartori@gmail.com)

M.R.S., 0000-0003-3793-2955; E.W.T., 0000-0002-4122-6511; A.S.A., 0000-0002-6765-8726; D.A.C., 0000-0001-9683-7013

Received 2 June 2018; Accepted 23 July 2018

Journal of Experimental Biology (2018) 221, jeb185967. doi:10.1242/jeb.185967

List of abbreviations

A–V diff	arteriovenous oxygen content difference
Ca_{O_2}	arterial oxygen content
Cv_{O_2}	venous oxygen content
CAM	chorioallantoic membrane
CO	cardiac output
COI	cardiac output index, product of heart rate and heart mass
f_H	heart rate
Hb	hemoglobin
Hct	hematocrit
n_H	Hill coefficient/cooperativity coefficient of hemoglobin oxygen binding
O_2 pulse	oxygen pulse, amount of O_2 consumed per heart beat
P_{50}	partial pressure of oxygen at 50% hemoglobin saturation
P_{O_2}	oxygen partial pressure
Pa_{O_2}	arterial partial pressure of oxygen
Pa_{CO_2}	arterial partial pressure of carbon dioxide
$\dot{V}_{O_2}$	oxygen consumption rate
Sa_{O_2}	hemoglobin oxygen saturation
$\%\dot{Q}$	relative blood flow distribution

while changes in oxygen affinity of the hemoglobin could also impact oxygen delivery (Tazawa and Mochizuki, 1977). This study is the first to investigate multiple aspects of convective oxygen transport during the embryonic development of an ectothermic vertebrate. To understand how convective oxygen transport in embryonic snapping turtles changes, we measured oxygen consumption ($\dot{V}_{O_2}$) and heart rate (f_H) and calculated oxygen pulse (O_2 pulse). We also analyzed blood collected from CAM arteries and veins to quantify blood oxygen content (Ca_{O_2} and Cv_{O_2}), hematocrit (Hct), hemoglobin concentration ([Hb]) and hemoglobin oxygen affinity (P_{50}). Finally, we determined relative blood flow ($\%\dot{Q}_{sys}$) and estimated cardiac output (CO) of the CAM. We hypothesized that as development progressed, embryonic snapping turtles would fuel an increase in metabolic rate by coordinated changes in convective transport, control of blood flow distribution and increasing levels of oxygen carrying capacity of the blood supplying the developing tissues.

MATERIALS AND METHODS

Eggs from common snapping turtles, *Chelydra serpentina* (Linnaeus 1758), were collected in Minnesota and transported to the Biology Department at the University of North Texas. Upon arrival, eggs were labeled, weighed and placed in plastic boxes (approximately 3 l volume), containing vermiculite mixed with water in a mass ratio of 1:1. Boxes were enclosed in plastic Ziploc® bags ventilated with humidified atmospheric air at 4 l min^{-1} to maintain the oxygen and water saturation at adequate levels. The bags were held in a walk-in environmental chamber set to 30°C. Water content of the vermiculite was maintained by weighing boxes three times a week and water was added as needed. A total of 104 eggs were used in this study. Eggs were taken at 50%, 70% and 90% incubation (total incubation 53 days), weighed and assigned for measurements of f_H and $\dot{V}_{O_2}$, collection of blood or injection of microspheres.

Embryonic f_H and $\dot{V}_{O_2}$ studies

Six embryos from each incubation time were used to determine f_H. Two silver wire electrodes (26 gauge) were inserted just under the surface of the shell of each egg, and then eggs were returned to incubation conditions overnight. The electrode leads were connected to an impedance converter (UFI 2991, Morro Bay, CA, USA) with the output signal connected to a data acquisition system (Powerlab model 8/35). Data were collected at 100 Hz using LabChart Pro (V 7.2, ADInstruments, Colorado Springs, CO, USA). f_H was recorded for up to 1 h in an environmental chamber at 30±0.5°C. The average of three 3 min periods over the final 15 min of the recording was used to establish f_H of each embryo.

The same embryos were then used to determine embryonic oxygen consumption, using a modified version of the closed system respirometry as previously outlined (Crossley et al., 2017b). Briefly, individual eggs were enclosed in hermetically sealed glass chambers (67 ml) with two ports, each connected to a three-way stopcock valve. The valves were closed for a period of 240 min at 50% incubation and for 60 min at 70% and 90% incubation. A 60 ml syringe was connected to one stopcock valve, which was opened for withdrawal of the chamber gas sample (20 ml). Air samples were drawn into a 2 m long length of PE-200 tubing open to the room air via another 3-way stopcock valve (a 'reservoir/sipper' system; see fig. 1 in Warburton et al., 1995, for a schematic diagram of the system). The 3-way stopcock was then opened to the analyzers, and gas samples passed through a 10 cm drying tube (MLA0343, ADInstruments) in a modified desiccation chamber similar to a desiccant cartridge (MLA6024, ADInstruments). This was connected to the gas analyzers in series for measurement of O_2 (S-3A1, Thermox, Ametek, Berwyn, PA, USA) and CO_2 (CD-3A, Thermox, Ametek). The gas sample was drawn through the analyzers at a rate of 15 ml min^{-1}. The output from each analyzer was connected to a data acquisition system (Powerlab model 8/35, ADInstruments) and gas concentration data were recorded at 20 Hz using LabChart Pro acquisition software (V 7.2, ADInstruments). This procedure was repeated three times, with 10 min allowed between samples during which the chambers were opened to restore ambient gas concentrations. Mean $\dot{V}_{O_2}$ was calculated based on chamber volume and time. Mass-specific $\dot{V}_{O_2}$ (ml O_2 kg^{-1} min^{-1}) was calculated based on embryo mass, which was measured at the completion of all studies (see below). For each egg, oxygen pulse (O_2 pulse) was calculated as the amount of whole-egg $\dot{V}_{O_2}$ per f_H and mass-specific O_2 pulse as mass-specific $\dot{V}_{O_2}$ per f_H.

Blood analysis studies

A different group of embryos was used for blood analysis studies. Eggs were removed from incubation and candled to locate either a tertiary artery carrying mixed oxygenated and deoxygenated blood or a vein in the CAM carrying oxygenated blood. Eggs were placed in holders (4 cm diameter) and moved to a temperature-controlled surgical chamber at 30±0.5°C. A portion of the eggshell was removed (~1 cm^2) and the targeted chorioallantoic artery or vein was occlusively cannulated under a dissection microscope (Leica MZ6, Leica Microsystems, Waukegan, IL, USA) using a heat-pulled polyethylene tube (PE-50) filled with 0.9% saline with 50 IU ml^{-1} heparin, as previously described (Crossley and Altimiras, 2000). A blood sample (approximately 50–80 µl) was immediately taken with a 100 µl Hamilton syringe for analysis.

A fraction of the whole blood was transferred to a 50 µl capillary tube and centrifuged (13,000 rpm) for Hct determination (N=13 for 50% and 70% incubation, N=12 for 90% incubation). The remaining fraction, ranging from 11 to 20 µl, was added to 4 ml of Drabkin's solution and analyzed spectrophotometrically (Shimadzu UV-1800, Cole Parmer, IL, USA) for determination of [Hb] (N=10 for 50% incubation, N=12 for 70% incubation and N=11 for 90% incubation). Fractions of the blood collected from CAM arteries of embryos at 70% and 90% incubation (N=5) were transferred to 60 µl capillaries, and analyzed in a previously

calibrated automatic blood gas analysis system (StatProfile pHOx Plus L, Nova Biomedical, Waltham, MA, USA) to measure blood gases (arterial partial pressure of O_2 and CO_2: Pa_{O_2} and Pa_{CO_2}).

For measurement of oxygen content (Tucker, 1967), a fraction of 8–20 µl of either an arterial or a venous blood sample was immediately inserted into a water-jacketed chamber (1.52 ml volume) containing an oxygen electrode (Radiometer, Copenhagen, Denmark) filled with degassed ferrocyanite solution, maintained at 30°C (±0.5°C) via a circulating water bath (VWR International, LLC, West Chester, PA, USA). The oxygen electrode was connected to a PHM 73 gas analyzer (Radiometer) and calibrated with degassed ferrocyanite solution (Tucker, 1967). Three oxygen partial pressure (P_{O_2}) values were recorded, immediately before the injection of the sample into the chamber and after 1 and 2 min. The difference between the initial P_{O_2} value and the mean after injection was used for the calculation of oxygen content (ml O_2 100 ml^{-1} blood) according to the equation proposed by Tucker (1967). Blood oxygen content values from vessels afferent to and efferent from the CAM were expressed as arteriovenous difference (A–V diff) and used to calculate total blood flow (CO) through the CAM (see below).

From a different group of embryos (7 at 50% and 70% incubation, 8 at 90% incubation), a 50 µl blood sample was diluted with 5 ml of Hemox solution, a manufacturer-provided buffer, and drawn into a cuvette for analysis by an automatic blood oxygen dissociation analyzer (Hemox Analyzer, model B, TCS, New Hope, PA, USA) to determine oxygen binding curves. The system was maintained at 30°C with a circulating water bath (VWR International, LLC). After air calibration, the sample was equilibrated with a gas mixture of O_2 with either 2% or 6% CO_2 (G400, Qubit, Kingston, ON, Canada) to simulate, respectively, arterial and venous CO_2 conditions. After air calibration of the P_{O_2} value, the sample was deoxygenated with nitrogen, until P_{O_2} decreased below 0.3 kPa. The output signal was connected to a data acquisition system (Powerlab model 8/35, ADInstruments) at 20 Hz using LabChart Pro acquisition software (V 7.2, ADInstruments). Calculation of the Bohr shift was based on $\Delta\log P_{50}/\Delta$logpH under the different conditions of CO_2. We considered that pH would not vary considerably under different Hb–O_2 saturations and used pH values measured with blood collected from 90% embryos diluted in the Hemox buffer, which were 7.17 under 2% CO_2 and 6.94 under 6% CO_2.

After all measurements and blood collection, embryos were killed with an overdose of isoflurane for measurement of mass of the embryo, heart, liver and yolk to the nearest 0.01 g. Embryonic stage was confirmed by comparison with the staging table of Yntema (1968) for *C. serpentina* embryos. At 50% of the incubation period, embryos corresponded to stages 19–20, at 70% to stages 23–24 and at 90% to stage 25. Relative cardiac index (relative COI) was calculated as the product of heart rate and heart mass corrected for embryonic body mass.

Regional blood flow measured by injection of microspheres

A separate group of embryos at each incubation time (5 at 50% incubation, 18 at 70% incubation and 15 at 90% incubation) were injected with colored polystyrene microspheres (Dye Track, Triton Technologies, San Diego, CA, USA) to measure regional blood flow. The microspheres were 15 µm in diameter, larger than the reported size of the snapping turtle red blood cells (Frair, 1977). Instrumentation was similar to that previously reported by our group. Briefly, a tertiary vein of the CAM was catheterized for injection of microspheres as described earlier. Microspheres were suspended in 0.9% saline containing 0.05% Tween 80 (to prevent agglomeration of the microspheres) at a final concentration of 1500 spheres μl^{-1}. Because of embryonic volume load limitation, a total of 52,500 yellow microspheres were injected at 50% incubation and a total of 75,000 at 70% and 90%. The injections were performed with a 100 µl glass Hamilton syringe into the catheterized vein, after a period of stabilization following the microsurgery (approximately 1 h). At the end of the protocol, a blood sample was withdrawn and stored in a 15 ml Falcon tube in order to detect whether any microspheres remained in the circulation. Embryos were killed with an intravenous dose of pentobarbital (50 µg kg^{-1}). Whole embryo, CAM and yolk membrane were immediately dissected, weighed and stored in either 15 or 50 ml Falcon tubes. The protocol for recovery of microspheres is described in detail in the guidelines provided by Triton Technologies Inc. (Mansfield, MA, USA) and summarized by Stecyk and colleagues (2004). We primarily used the sedimentation method based on a series of centrifugations. Briefly, the sedimentation recovery procedure consists of the following steps: alkaline digestion, a series of washes (Triton X-100, acidified ethanol and ethanol) and elution of the dye. We started tissue digestion with 1 mol l^{-1} KOH (Sigma-Aldrich, St Louis, MO, USA) and added 10,000 blue microspheres to each tube to assess the effectiveness of the recovery process.

Tissues were sonicated to accelerate digestion, using an ultrasonic homogenizer (Fisher Scientific, Waltham, MA, USA), at 70% of full power for 30 s. The digestion step was repeated until a tissue pellet was no longer visible. Samples containing calcified tissue were subjected to additional treatment with a bone-digesting reagent (0.12% EDTA, 5.38% HCl, 94% H_2O). For tissues that were not digested after several repetitions of sonication, vortexing and alkaline digestion (particularly yolk and whole-embryo samples), a vacuum filtration method using a 25 mm diameter filter with a 10 µm pore size was applied (Triton Technologies Inc., part #31079).

After digestion, the samples were subjected to a series of washes, and the colored dye was eluted from the microspheres with acidified Cellosolve acetate (Sigma-Aldrich). Subsamples of each eluted sample (175 µl) were then transferred to a crystal 96-well plate for dye analysis using a spectrophotometer (Synergy H1, Biotek, VT, USA) at absorbance wavelengths of 650 nm for blue spheres and 440 nm for yellow spheres. To calculate total microspheres and recovery rates for each sample, we entered the absorbance values at each wavelength from each tube into a calculation Excel file, provided by the manufacturer. We calculated fractions of blood flow ($\%\dot{Q}_{sys}$) directed to the vascular bed of the embryo, CAM and yolk, considering the total microspheres recovered from the tissues of individual eggs and correcting for the microsphere recovery rate accessed by the blue control spheres.

Estimation of Hb saturation and CAM blood flow

By substituting our measured arterial oxygen content (Ca_{O_2}), hemoglobin concentration ([Hb] in g dl^{-1}) and oxygen partial pressure (Pa_{O_2}) at 70% and 90% into the oxygen content equation Ca_{O_2}=[Hb]×1.34 ml O_2 g^{-1} Hb×Sa_{O_2}+Pa_{O_2}×0.003 ml O_2 $mmHg^{-1}$ dl^{-1}, we estimated hemoglobin oxygen saturation (Sa_{O_2}).

By combining our measured CAM A–V diff with the measured values for whole-egg $\dot{V}_{O_2}$ or mass-specific $\dot{V}_{O_2}$, we estimated CAM blood flow ($\dot{Q}_{CAM}$) using the Fick equation ($\dot{V}_{O_2}$=CO×A–V diff). Then, $\dot{Q}_{CAM}$ was determined as the mean $\dot{V}_{O_2}$ calculated from one group of embryos divided by the A–V diff calculated with a different group of embryos.

Journal of Experimental Biology (2018) 221, jeb185967. doi:10.1242/jeb.185967

Statistical analysis

Data from oxygen equilibrium curves were plotted as Hill allosteric curves using GraphPad Prism® software. To measure Hb–O_2 affinity, data were fitted to linear regressions ($r^2 \geq 0.95$) in which P_{O_2} at 50% Hb saturation (P_{50}) and the corresponding cooperativity coefficient (n_H) corresponded to the zero intercept and slope, respectively, of Hill plots $\{\log[Y/(1-Y)]\}$ versus $\log P_{O_2}$ (where Y is the fractional saturation) fitted to seven saturation steps between 20% and 80%.

All data were tested for differences between the incubation periods using parametric one-way ANOVA but whenever data failed normality or homoscedasticity we used the non-parametric ANOVA on ranks. *Post hoc* Student–Newman–Keuls (SNK) or Dunn's tests were used for detection of differences across groups. For oxygen content, a *t*-test was used to account for differences between arterial and venous blood. The level of significance was established as $P<0.05$ and data are presented as means± s.e.m. All statistical analyses were conducted with Sigma Plot V. 11 software.

RESULTS

Egg mass did not differ between the incubation periods sampled (mean egg mass=12.9±0.2 g; Table 1), embryonic yolk-free body mass increased 4.4-fold from 1.62±0.08 g at 50% incubation to 7.16±0.16 g at 90% incubation (one-way ANOVA+SNK; $P<0.001$; Table 1). Liver also increased 4.5-fold from 0.047±0.002 g to 0.213±0.008 g, whereas heart mass increased 3-fold from 0.007± 0.0002 g to 0.022±0.001 g during the same period (one-way ANOVA+SNK; $P<0.001$; Table 1). Relative heart mass decreased from 0.46±0.02% to 0.31±0.02% (one-way ANOVA+SNK; $P<0.001$; Table 1).

f_H decreased from 56±2 beats min^{-1} at 50% incubation to 43± 3 beats min^{-1} at 90% incubation (one-way ANOVA+SNK; $P<0.001$; Fig. 1A) whereas $\dot{V}_{O_2}$ of whole eggs increased continuously from $8.5\times10^{-3}\pm5\times10^{-4}$ ml O_2 egg^{-1} min^{-1} at 50% incubation to $19.9\times10^{-3}\pm7\times10^{-4}$ ml O_2 egg^{-1} min^{-1} at 90% incubation (one-way ANOVA+SNK; $P<0.001$; Fig. 1B). Mass-specific $\dot{V}_{O_2}$ decreased progressively from 6.0±0.4 ml O_2 kg^{-1} min^{-1} at 50% incubation to 2.8±0.1 ml O_2 kg^{-1} min^{-1} at 90% incubation (one-way ANOVA+SNK; $P<0.001$; Fig. 1C) as embryonic mass increased. Oxygen pulse, the ratio of oxygen consumed per heart beat, increased from $1.5\times10^{-4}\pm1\times10^{-5}$ ml O_2 $beat^{-1}$ at 50% incubation to $5.0\times10^{-4}\pm4\times10^{-5}$ ml O_2 $beat^{-1}$ at 90% incubation (one-way ANOVA+SNK; $P<0.001$; Fig. 1D). When calculated with mass-specific $\dot{V}_{O_2}$, mass-specific O_2 pulse decreased from 0.11 ml O_2 $beat^{-1}$ kg^{-1} to 0.07 ml O_2 $beat^{-1}$ kg^{-1} (one-way ANOVA+SNK; $P<0.001$).

Table 1. Changes in mass of snapping turtle embryos at 50%, 70% and 90% incubation

Mass	50%	70%	90%
Egg (g)	12.4±0.5[a]	13.1±0.4[a]	13.4±0.2[a]
Yolk (g)	3.72±0.15[a]	2.71±0.13[b]	1.18±0.07[c]
Body (g)	1.62±0.08[a]	4.39±0.13[b]	7.16±0.16[c]
Heart (g)	0.007±0.0002[a]	0.017±0.001[b]	0.022±0.001[c]
Heart/body (%)	0.46±0.02[a]	0.38±0.01[b]	0.31±0.02[c]
Liver (g)	0.047±0.002[a]	0.111±0.006[b]	0.213±0.008[c]
N	21	24	21

Data are presented as means±s.e.m. Different letters denote statistical differences among incubation periods.

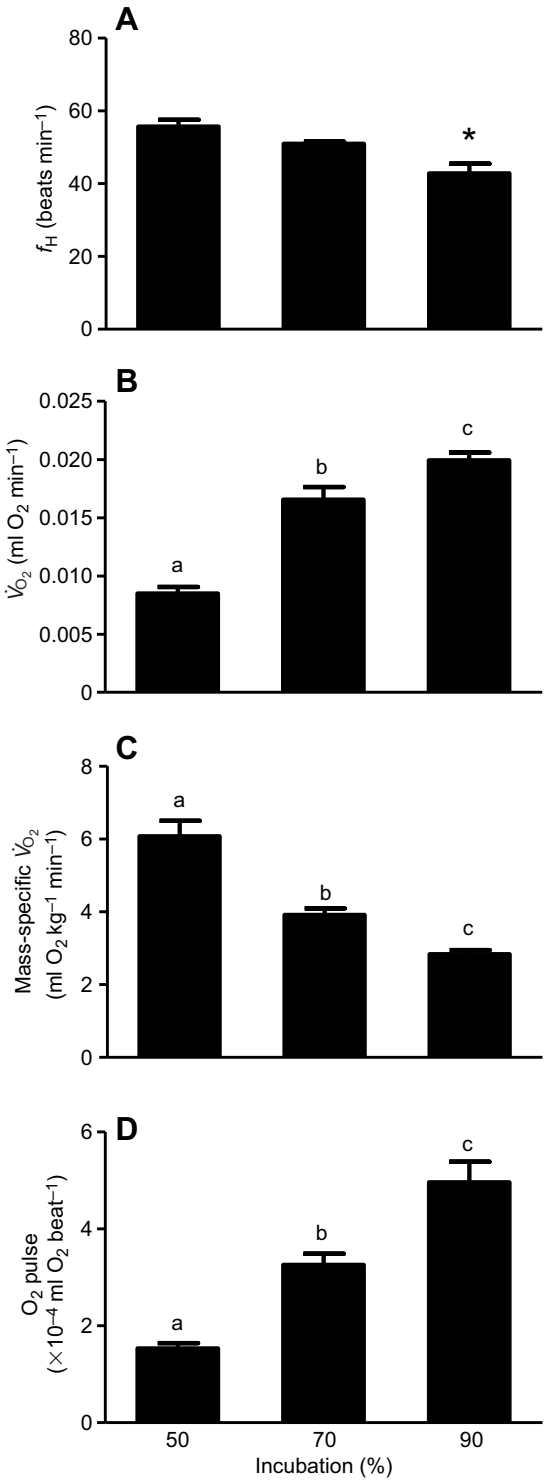

Fig. 1. Heart rate (f_H), oxygen consumption ($\dot{V}_{O_2}$), mass-specific $\dot{V}_{O_2}$ and O_2 pulse from snapping turtles at 50%, 70% and 90% incubation. (A) Mean (+s.e.m.) f_H of embryonic turtles at different times in the incubation period. The rate at 90% incubation is lower than that at 50% and 70% (*$P<0.001$). (B) Total $\dot{V}_{O_2}$ of *Chelydra serpentina* eggs at 50%, 70% and 90% of the incubation period. The volume of oxygen consumed increased progressively throughout the incubation period ($P<0.001$). (C) Embryonic mass-specific $\dot{V}_{O_2}$. The rate of oxygen consumption decreased progressively with the increase in embryonic mass ($P<0.001$). (D) Oxygen pulse calculated from $\dot{V}_{O_2}$ and f_H data. Oxygen pulse increased progressively at 70% and 90% incubation ($P<0.001$). Different letters in B–D indicate a significant difference between values.

Blood values

Hct and Hb did not change between incubation periods and were 22.4±1.3 and 9.5±0.4 ml O_2 100 ml^{-1} blood, respectively (Table 2). Partial pressure of blood gases, Pa_{O_2} and Pa_{CO_2}, from CAM arteries containing mixed oxygenated and deoxygenated blood also did not differ during the periods measured (70% and 90%; Table 2).

Blood O_2 content from the CAM artery, Ca_{O_2}, did not differ between the incubation periods studied (mean of 0.9±0.1 ml O_2 100 ml^{-1} blood; ANOVA on ranks; P=0.824) but CAM venous blood O_2 content, Cv_{O_2}, increased from 2.7±0.4 ml O_2 100 ml^{-1} blood at 50% incubation to 5.0±0.5 ml O_2 100 ml^{-1} blood at 90% incubation (one-way ANOVA+SNK; P<0.05), resulting in a 2-fold increase in A–V diff (see Fig. 2).

Oxygen equilibrium curves did not differ between 2% and 6% CO_2 conditions in all incubation periods, indicating the lack of a marked Bohr shift (F=0.47; P=0.7; Table 2, Fig. 3). At 50% incubation, we found two patterns of dissociation curves, which reflected different embryonic stages, although they did not differ statistically in embryonic mass (Table 2). Therefore, the period was divided into two subgroups: 'early', which was equivalent to stage 19 of development (50%–E) and 'late', which was equivalent to stage 20 of development (50% – L). Late 50% presented a dissociation curve pattern similar to that at 70% and 90% incubation and also had similar P_{50} values. Early 50% had a right-shifted curve and a higher P_{50} (lower oxygen affinity) when compared with the late 50%, 70% and 90% incubation (one-way ANOVA+SNK; P<0.0001; Table 2, Fig. 3). Hill coefficients (n_H) for 2% and 6% CO_2 curves were all positive (>1) and did not differ between the incubation periods, indicating no significant change in the level of hemoglobin cooperativity (one-way ANOVA+SNK; P=0.41; Table 2).

Regional blood flow

The distribution of microspheres revealed that relative blood flow directed to the embryonic tissues (%$\dot{Q}_{body}$), to the chorioallantoic membrane (%$\dot{Q}_{CAM}$) and to the yolk sac (%$\dot{Q}_{yolk}$) differed with incubation time (one-way ANOVA+SNK; P<0.0001; Fig. 4). The blue control spheres added to determine microsphere loss during tissue processing revealed a high efficiency of the recovery process, with rates of 89.76±0.02% at 50% incubation, 101.79±0.02 at 70% incubation and 103.30±0.02 at 90% incubation.

Throughout the last half of incubation the percentage of blood flow directed to embryonic tissues (%$\dot{Q}_{body}$) was always greater than the flow to the CAM or to the yolk (Fig. 4). %$\dot{Q}_{body}$ was maximal at 50% incubation (84%) and minimal at 70% incubation (66%) (Fig. 4A,B). The percentage of blood flow directed to the CAM was initially low (9%) at 50% incubation then rose to 31% and fell to 25% between 70% and 90% incubation (Fig. 4). The relative blood flow directed to the yolk sac was 7% at 50% incubation and progressively decreased upon its depletion (Fig. 4), with the small volume of yolk remaining being incorporated into the abdominal cavity before hatching.

Estimation of CAM blood flow ($\dot{Q}_{CAM}$) and Hb saturation (Sa_{O_2})

By substituting our measured parameters at 70% and 90% into the equation Ca_{O_2}=[Hb]×1.34 ml O_2 g Hb^{-1}×Sa_{O2}+Pa_{O_2}×0.003 ml O_2 $mmHg^{-1}$ dl^{-1}, we were able to estimate Hb oxygen saturation (Sa_{O_2}), which increased from 34% to 49% (Table 2).

When we inserted our $\dot{V}_{O_2}$ and A–V diff data in the Fick equation (CO=$\dot{V}_{O_2}$/A−V diff) we found that blood flow through the CAM ($\dot{Q}_{CAM}$) increased from 0.46 ml min^{-1} at 50% incubation to 0.71 ml min^{-1} at 70% incubation, but then decreased to 0.50 ml min^{-1} at 90% (Fig. 4, Table 2). However, when using mass-specific $\dot{V}_{O_2}$, $\dot{Q}_{CAM}$ decreased from 0.33 ml min^{-1} g^{-1} at 50% incubation to 0.07 ml min^{-1} g^{-1} at 90% incubation (Fig. 4, Table 2). In agreement with this last finding, the relative COI also indicated a 50% decrease in total cardiac output from 50% to 90% incubation (Table 2).

DISCUSSION

The development of the components of the convective oxygen transport system in relation to changes in metabolic rate were largely unknown in reptilian embryos. In this study, we found that blood properties were relatively constant throughout snapping turtle incubation, while indexes of cardiac output, relative heart mass

Table 2. Blood oxygen carrying capacity properties and chorioallantoic membrane (CAM) cardiac output from snapping turtle embryos at 50%, 70% and 90% incubation

	50%		70%	90%
Hct (%)	23.5±1.4 (13)[a]		22.7±1.5 (13)[a]	21.1±0.9 (12)[a]
[Hb] (mg dl^{-1})	6.8±0.2 (10)[a]		7.0±0.4 (12)[a]	7.5±0.4 (11)[a]
Pa_{O_2} (kPa)	–		3.0±0.2[a]	2.6±0.3[a]
Pa_{CO_2} (kPa)	–		3.2±0.2[a]	3.4±0.3[a]
Sa_{O_2} (%)	–		34% (5)	49% (5)
Relative COI	0.28±0.10[a]		0.17±0.04[b]	0.14±0.05[b]
%$\dot{Q}_{CAM}$	9.2±2.3 (5)		31.6±3.7 (18)	25.3±6.2 (15)
$\dot{Q}_{CAM}$ (ml min^{-1})	0.46		0.71	0.50
$\dot{Q}_{CAM}$ (ml min^{-1} g^{-1})	0.33		0.17	0.07
	50% – E (3)	50% – L (4)	70% (7)	90% (8)
Embryo mass (g)	1.8±0.5[a]	2.3±0.5[a]	4.4±0.3[b]	7.0±0.1[c]
P_{50} at 2% CO_2 (kPa)	6.72±0.69[a]	1.35±0.11[b]	1.25±0.04[b]	1.25±0.05[b]
P_{50} at 6% CO_2 (kPa)	6.25±1.49[a]	1.72±0.15[b]	1.67±0.08[b]	1.63±0.05[b]
Bohr shift	–0.19±0.10[a]	–0.47±0.16[a]	–0.46±0.08[a]	–0.49±0.15[a]
n_H at 2% CO_2	2.1±0.1[a]	2.1±0.2[a]	2.2±0.1[a]	2.4±0.1[a]
n_H at 6% CO_2	1.8±0.3[a]	2.0±0.5[a]	2.1±0.1[a]	2.4±0.1[a]

Hct, hematocrit; [Hb], hemoglobin concentration; Pa_{O_2}, arterial partial pressure of oxygen; Pa_{CO_2}, arterial partial pressure of carbon dioxide; Sa_{O_2}, hemoglobin oxygen saturation; relative COI, cardiac output index calculated based on cardiac mass; %$\dot{Q}_{CAM}$, proportion of cardiac output directed to the CAM calculated by the microsphere distribution; $\dot{Q}_{CAM}$, cardiac output calculated with the Fick equation; P_{50}, partial pressure of oxygen at 50% Hb saturation; n_H, Hill coefficient. Data derived from the oxygen dissociation curves at 50% incubation (P_{50}, Bohr shift and n_H) were divided in two subgroups, early (50% – E) and late (50% – L). All data are presented as means±s.e.m. Different letters denote statistical significance among incubation periods; sample size is given in parentheses.

Journal of Experimental Biology (2018) 221, jeb185967. doi:10.1242/jeb.185967

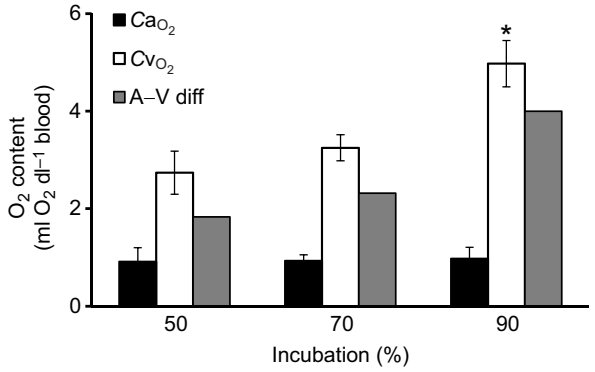

Fig. 2. Blood oxygen content of embryonic snapping turtles at 50%, 70% and 90% incubation. Mean blood oxygen content in arteries (Ca_{O_2}) and veins (Cv_{O_2}) of the choriollantoic membrane of snapping turtle embryos, and the resulting arteriovenous difference (A–V diff). Ca_{O_2} did not vary through development (P=0.824), but Cv_{O_2} increased at 90% of development (*P<0.05). Ca_{O_2} was lower than Cv_{O_2} at every incubation period tested (t-test; P<0.02).

and mass-specific metabolic rate decreased over the course of incubation. If this pattern persists during the pre-hatching period (>90% of incubation), it could account for previously reported patterns of whole-egg $\dot{V}_{O_2}$ in snapping turtle embryos.

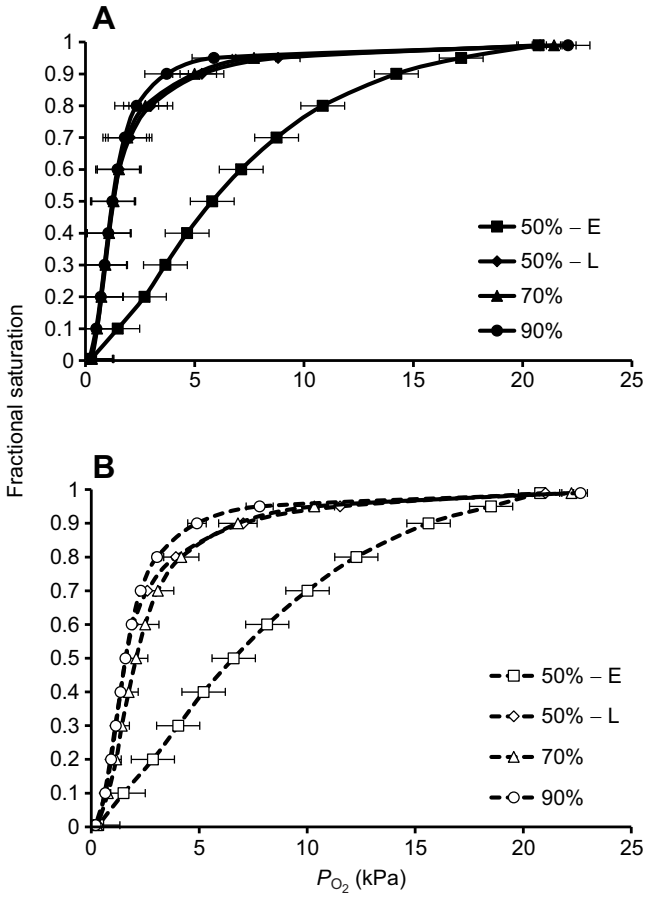

Fig. 3. Oxygen equilibrium curves from snapping turtles at 50%, 70% and 90% incubation at different CO_2 conditions. Samples were deoxygenated with N_2 mixed with (A) 2% CO_2 (similar to oxygenated blood) or (B) 6% CO_2 (similar to deoxygenated blood) and the saturation calculated from the fraction of deoxyhemoglobin. Data are shown for early 50% (50% – E), late 50% (50% – L), 70% (triangles) and 90% (circles) incubation.

f_H of snapping turtle embryos decreased significantly at the end of incubation, a common pattern of members of the order Testudines (Alvine et al., 2013; Birchard and Reiber, 1996; Crossley, 1999; Birchard, 2000; McGlashan et al., 2015; Taylor et al., 2014) and in contrast to the relatively constant f_H during incubation of Squamata (Birchard and Reiber, 1996; Nechaeva et al., 2007; Du et al., 2009; Sartori et al., 2017). In snapping turtles, f_H reduction has been related to the onset of parasympathetic tone, which is present at 70% incubation (Alvine et al., 2013), in comparison to the late onset of vagal tone found in green iguana (Sartori et al., 2015) and the lack of vagal tone during incubation in the American alligator (Eme et al., 2011). f_H is a critical variable in the adjustment of cardiac output during periods of increased metabolic demand (Joyce et al., 2018) and its decrease, coupled to the appearance of parasympathetic control, may reflect an overall reduction in tissue demands. Mass-specific metabolic rate did fall at 50% and 90% incubation, supporting this speculation (Fig. 1C).

Snapping turtle embryos markedly increased in body mass (4.4-fold) during the second half of incubation concurrent with the depletion of the yolk (Table 1). To support this growth, egg $\dot{V}_{O_2}$ doubled during the last half of the incubation period but f_H decreased by 23%, which resulted in a 3-fold increase in O_2 pulse. Our previous study in a squamate reptile showed that $\dot{V}_{O_2}$ varied independently of f_H (Sartori et al., 2017), indicating that other physiological mechanisms were involved in matching O_2 supply to tissue demand during embryonic incubation. In the present study, heart mass tripled from 50% to 90% incubation (Table 1) and this was coupled to an increase in oxygen pulse (Fig. 1D). However, the size of the heart relative to the size of the embryo decreased from 0.46% at 50% incubation to 0.31% at 90% incubation (Table 1). This is also the case for the turtles *Emys orbicularis* (from approximately 0.56% at 50% incubation to 0.31% when close to hatching; Nechaeva et al., 2007) and *Lepidochelys olivacea* (from 0.46% at 70% incubation to 0.39% at 90%; Crossley et al., 2017a), and for the lizard *Iguana iguana* (from 0.35% at 30% incubation to 0.26% at 90% incubation; Sartori et al., 2017). This difference in heart growth, when compared with the body mass increase, could be offset to some extent by the reduction in tissue oxygen requirement of the embryo, reflected by the decrease in mass-specific $\dot{V}_{O_2}$ (Sartori et al., 2017) and a consequent decrease in mass-specific O_2 pulse, as described for the marine iguana by Butler and colleagues (2002).

Unlike prior studies, we found progressive increases in the $\dot{V}_{O_2}$ of snapping turtle eggs during the later stages of development (Fig. 1B). Previous reports of egg $\dot{V}_{O_2}$ for this species demonstrated that $\dot{V}_{O_2}$ reached a maximum value before rapidly declining immediately prior to hatching (Gettinger et al., 1984; Miller and Packard, 1992; Birchard and Reiber, 1995). While our findings differed from this, we did not measure $\dot{V}_{O_2}$ during the final 10% of incubation, which likely contributed to the apparent contradiction with prior work.

Venous blood leaving the CAM, the site of gas exchange, carried more O_2 in embryos at 90% incubation (Fig. 2), which would support the increase in total egg $\dot{V}_{O_2}$ (Fig. 1B). Factors that would enable the increase in oxygen carrying content of the venous blood could be: (i) an increase in the number of red blood cells or in Hb concentration; (ii) an increased saturation of the Hb, related to the modulation of Hb oxygen affinity; (iii) changes in the level of allantoic shunting, reducing the levels of deoxygenated blood mixed with the oxygenated blood; (iv) increases in CAM vascularization; and (v) decreases in diffusion resistance barrier. We were unable to monitor levels of shunting but found that Hct and

Journal of Experimental Biology (2018) 221, jeb185967. doi:10.1242/jeb.185967

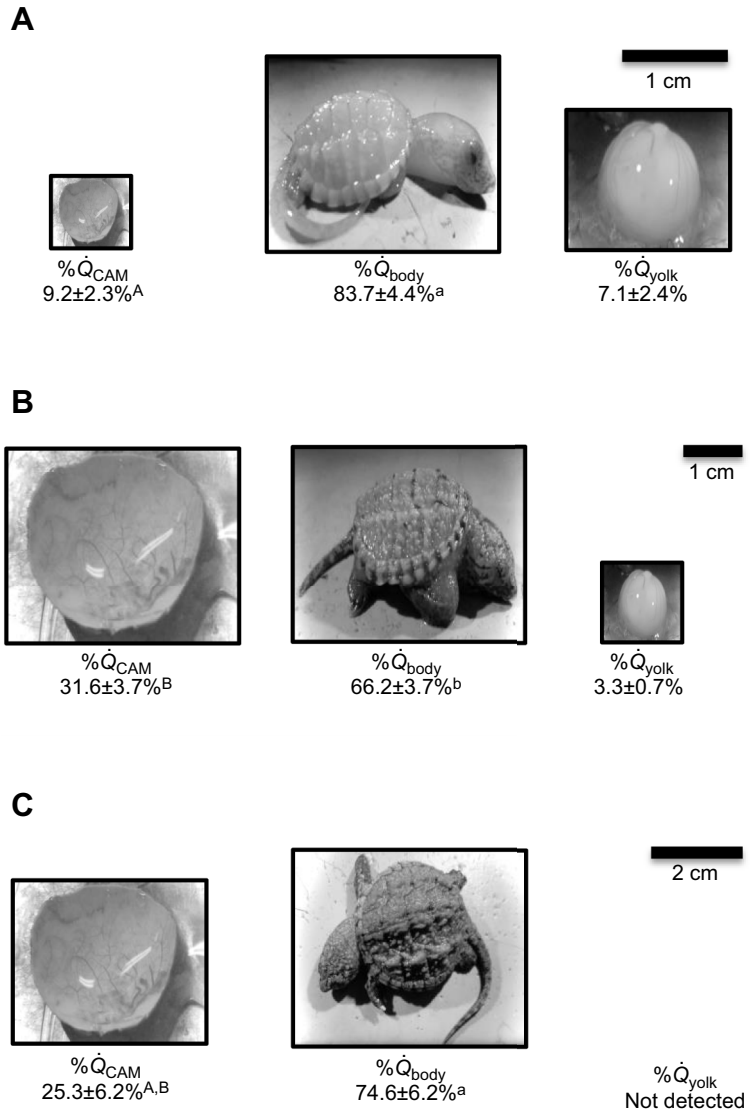

Fig. 4. Relative cardiac output distribution in embryonic snapping turtles at 50%, 70% and 90% incubation. Percentages of relative blood flow or systemic cardiac output (%$\dot{Q}_{sys}$): blood flow to embryonic tissues (%$\dot{Q}_{body}$); blood flow to the chorioallantoic membrane (%$\dot{Q}_{CAM}$); and blood flow to the yolk sac (%$\dot{Q}_{yolk}$) during routine normoxia at 30°C. (A) 50% incubation (*N*=5), (B) 70% incubation (*N*=18 for %$\dot{Q}_{CAM}$ and %$\dot{Q}_{body}$, and *N*=11 for %$\dot{Q}_{yolk}$) and (C) 90% incubation (*N*=15). Values of %$\dot{Q}_{sys}$ were obtained with the microsphere study. The different sizes of the yolk and CAM images are to illustrate the different fractions of %$\dot{Q}_{sys}$. Scale bars are depicted in each figure. Different uppercase/lowercase letters indicate a significant difference between values.

Hb content remained unchanged throughout the last half of development. Further, with the exception of early 50% incubation embryos, P_{50} was constant during the last half of the incubation (Table 2, Fig. 3). Calculated Hb saturation at 90% incubation was 15% higher than that at 70%, which likely contributed to the increase in blood oxygen content of blood returning from the CAM (Table 2). While physical measures of CAM development were not determined in our study, prior work reported that the CAM completely encloses the egg at approximately 60–70% incubation (Webb et al., 1987; Stewart and Florian, 2000; Nechaeva et al., 2007). Nevertheless, CAM mass can continue to increase thereafter, suggesting an expansion of the vascularization (Birchard and Reiber, 1993; Kam, 1993; Corona and Warburton, 2000; Blackburn et al., 2003). An increase in CAM vascularization late in incubation would then support the calculated increase in Hb saturation and allow greater surface area for oxygen loading, which would also impact the overall increase in egg $\dot{V}_{O_2}$ (Fig. 1B). The relative cardiac output measurements showed that during the second half of incubation the fraction of CO directed to the yolk was very small, further increasing the total amount flowing to embryonic tissues (Fig. 4). Over the final 30% of development, the CAM vasculature received a considerably higher fraction (25–32%) of CO, when compared with that at 50% incubation (Fig. 4). In comparison to other vertebrate groups, this value was lower than that reported for late-stage chicken embryos (44%; Mulder et al., 1997) and for the placenta fraction in near-term fetal sheep (41%; Jensen et al., 1991); however, this could be attributed to differences in developmental temperature and overall metabolic demand. The increase in CO directed to the CAM from 50% to 70% incubation in snapping turtles (Fig. 4A,B) may reflect a higher vascular density and an expanded surface for gas exchange to occur. The majority of CO was directed to the embryo at all stages measured, although it was reduced at 70% incubation in comparison to that at 50% and 90% incubation (Fig. 4). It is important to note that absolute values of blood flow to the organs were not determined because of limitations of the microsphere technique as reported by Mulder and colleagues (1997). The size of the snapping turtle embryos and their small blood volume restricted the collection of a reference blood sample simultaneously with microsphere injection and absolute measures of blood flow proved unsuccessful.

Our estimates of CAM blood flow suggest an overall decrease at 90% incubation (Table 2). Also, the calculated relative cardiac output

index indicated that mass-specific cardiac output decreased throughout incubation, which was previously suggested to occur in developing turtles (Birchard and Reiber, 1996; Crossley and Burggren, 2009; Crossley et al., 2017a). This reduction could contribute to a slowing, a plateau or a decline in oxygen consumption previously reported for embryonic turtles (Ackerman, 1981; Booth and Astill, 2001; Reid et al., 2009; Thompson, 1993). In this study, we found that the estimated CO decreased with the progressive increase in egg $\dot{V}_{O_2}$; however, embryonic mass-specific $\dot{V}_{O_2}$ decreased as well (Fig. 1C). Nevertheless, the increase in oxygen carrying capacity of the blood and the lower mass-specific $\dot{V}_{O_2}$ at late stages of development compensate for any CO decline in snapping turtles and therefore it would not compromise metabolic function.

In summary, our findings indicate that snapping turtle embryos increase oxygen carrying capacity while COI and f_H decrease late in development. While we lack sufficient data to definitively assign the change in mass-specific metabolic rate to changes in convective oxygen transport capacity, our data do suggest that the two are correlated. If this pattern persisted into the final 10% of snapping turtle incubation, it may contribute to the previously reported patterns of whole-egg $\dot{V}_{O_2}$ during the final stages of embryonic development.

Acknowledgements
We thank Prof. Turk Rehn for aid with egg collection and Dr Kevin Tate for help in egg and animal care.

Competing interests
The authors declare no competing or financial interests.

Author contributions
Conceptualization: E.W.T., D.A.C.; Methodology: M.R.S., Z.F.K., E.W.T., D.A.C.; Formal analysis: M.R.S.; Investigation: M.R.S., Z.F.K., D.A.C.; Data curation: M.R.S., D.A.C.; Writing - original draft: M.R.S.; Writing - review & editing: M.R.S., Z.F.K., E.W.T., A.S.A., D.A.C.; Supervision: E.W.T., A.S.A., D.A.C.; Project administration: M.R.S., E.W.T., A.S.A., D.A.C.; Funding acquisition: A.S.A., D.A.C.

Funding
This study was supported by the São Paulo Research Foundation (Fundação de Amparo a Pesquisa do Estado de São Paulo, FAPESP; no. 2013/05677-9 to A.S.A./M.R.S.; no. 2012/06938-8 to A.S.A./E.W.T.) and the National Science Foundation (NSF IBN-IOS 0845741 to D.A.C.). E.W.T. was a Visiting Researcher with the Science Without Borders Programme (Conselho Nacional de Desenvolvimento Científico e Tecnológico, CNPq; 401061/2014-0 to F. T. Rantin/E.W.T.).

References
Ackerman, R. A. (1981). Oxygen consumption by sea turtle (Chelonia, Caretta) eggs during development. *Physiol. Zool.* **54**, 316-324.
Alvine, T., Rhen, T. and Crossley, D. A., II. (2013). Temperature-dependent sex determination modulates cardiovascular maturation in embryonic snapping turtles *Chelydra serpentina*. *J. Exp. Biol.* **216**, 751-758.
Aulie, A. and Kanui, T. I. (1995). Oxygen consumption of eggs and hatchlings of the Nile crocodile (*Crocodylus niloticus*). *Comp. Biochem. Physiol. A Physiol.* **112**, 99-102.
Birchard, G. F. (2000). An ontogenetic shift in the response of heart rates to temperature in the developing snapping turtle (*Chelydra serpentina*). *J. Therm. Biol.* **25**, 287-291.
Birchard, G. F. and Reiber, C. L. (1993). A comparison of avian and reptilian chorioallantoic vascular density. *J. Exp. Biol.* **178**, 245-249.
Birchard, G. F. and Reiber, C. L. (1995). Growth, metabolism, and chorioallantoic vascular density of developing snapping turtles (*Chelydra serpentina*): influence of temperature. *Physiol. Zool.* **68**, 799-811.
Birchard, G. F. and Reiber, C. L. (1996). Heart rate during development in the turtle embryo: effect of temperature. *J. Comp. Physiol. B* **166**, 461-466.
Blackburn, D. G., Johnson, A. R. and Petzold, J. L. (2003). Histology of the extraembryonic membranes of an oviparous snake: towards a reconstruction of basal squamate patterns. *J. Exp. Zool.* **299A**, 48-58.
Booth, D. T. (1998a). Incubation of turtle eggs at different temperatures: do embryos compensate for temperature during development? *Physiol. Zool.* **71**, 23-26.
Booth, D. T. (1998b). Effects of incubation temperature on the energetics of embryonic development and hatchling morphology in the Brisbane river turtle *Emydura signata*. *J. Comp. Physiol. B Biochem. Syst. Environ. Physiol.* **168**, 399-404.
Booth, D. T. and Astill, K. (2001). Incubation temperature, energy expenditure and hatchling size in the green turtle (*Chelonia mydas*), a species with temperature-sensitive sex determination. *Aust. J. Zool.* **49**, 389-396.
Booth, D. T. and Thompson, M. B. (1991). A Comparison of reptilian eggs with those of megapode birds. In *Egg Incubation: Its Effects in Embryonic Development in Birds and Reptiles* (ed. D. C. Deeming and M. W. J. Ferguson), pp. 325-345, Cambridge: Cambridge University Press.
Booth, D. T., Thompson, M. B. and Herring, S. (2000). How incubation temperature influences the physiology and growth of embryonic lizards. *J. Comp. Physiol.* **170B**, 269-276.
Burggren, W., Farrell, A. and Lillywhite, H. (2011). Vertebrate cardiovascular systems. In *Comprehensive Physiology*, Suppl. 30, *Handbook of Physiology, Comparative Physiology* (ed. R. Terjung). Hoboken, NJ: Wiley-Blackwell.
Butler, P. J., Frappell, P. B., Wang, T. and Wikelski, M. (2002). The relationship between heart rate and rate of oxygen consumption in Galapagos marine iguanas (*Amblyrhynchus cristatus*) at two different temperatures. *J. Exp. Biol.* **205**, 1917-1924.
Corona, T. B. and Warburton, S. J. (2000). Regional hypoxia elicits regional changes in chorioallantoic membrane vascular density in alligator but not chicken embryos. *Comp. Biochem. Physiol. A Mol. Integr. Physiol.* **125**, 57-61.
Crossley, D. A., II (1999). Development of cardiovascular regulation in embryos of the domestic fowl (*Gallus gallus*), with partial comparison to embryos of the desert tortoise (*Gopherus agassizii*). *PhD thesis*, University of North Texas, Denton, TX.
Crossley, D. A., , II and Altimiras, J. (2000). Ontogeny of autonomic control of cardiovascular function in the domestic chicken *Gallus gallus*. *Am. J. Physiol.* **279**, R1091-R1098.
Crossley, D. A., , II and Altimiras, J. (2005). Cardiovascular development in embryos of the American alligator *Alligator mississippiensis*: effects of chronic and acute hypoxia. *J. Exp. Biol.* **208**, 31-39.
Crossley, D. A., , II and Burggren, W. W. (2009). Development of cardiac form and function in ectothermic Sauropsids. *J. Morphol.* **270**, 1400-1412.
Crossley, D. A., , II, Smith, C., Harfush, M., Sánchez-Sánchez, H., Garduño-Paz, M. V. and Méndez-Sánchez, J. F. (2017a). Developmental cardiovascular physiology of the olive ridley sea turtle (*Lepidochelys olivacea*). *Comp. Biochem. Physiol.* **211A**, 69-76.
Crossley, D. A., , II, Ling, R., Nelson, D., Gillium, T., Conner, J., Hapgood, J., Elsey, R. M. and Eme, J. (2017b). Metabolic responses to chronic hypoxic incubation in embryonic American alligators (*Alligator mississippiensis*). *Comp. Biochem. Physiol. A Mol. Integr. Physiol.* **203**, 77-82.
Dmi'el, R. (1970). Growth and metabolism in snake embryos. *J. Embryol. Exp. Morph.* **23**, 761-772.
Du, W.-G., Radder, R. S., Sun, B. and Shine, R. (2009). Determinants of incubation period: do reptilian embryos hatch after a fixed total number of heart beats? *J. Exp. Biol.* **212**, 1302-1306.
Eme, J., Altimiras, J., Hicks, J. W. and Crossley, D. A., II. (2011). Hypoxic alligator embryos: chronic hypoxia, catecholamine levels and autonomic responses of in ovo alligators. *Comp. Biochem. Physiol. A Mol. Integr. Physiol.* **160**, 412-420.
Eme, J., Tate, K. B., Kohl, Z. F., Slay, C. E., Hicks, J. W. and Crossley, D. A., II. (2012). Cardiovascular plasticity during hypoxic development in reptile embryos. *Integr. Comp. Biol.* **52**, E54-E54.
Frair, W. (1977). Turtle red blood cells packed volumes, sizes and numbers. *Herpetologica* **33**, 167-190.
Gettinger, R. D., Paukstis, G. L. and Gutzke, W. H. N. (1984). Influence of hydric environment on oxygen consumption by embryonic turtles *Chelydra serpentina* and *Trionyx spiniferus*. *Physiol. Zool.* **57**, 468-473.
Jensen, A., Roman, C. and Rudolph, A. (1991). Effects of reducing uterine blood flow on fetal blood flow distribution and oxygen delivery. *J. Dev. Physiol.* **15**, 309-323.
Joyce, W., Elsey, R. M., Wang, T. and Crossley, D. A., II. (2018). Maximum heart rate does not limit cardiac output at rest or during exercise in the American alligator (*Alligator mississippiensis*). *Am. J. Physiol. Regul. Integr. Comp. Physiol.* **176**, 247.
Kam, Y.-C. (1993). Physiological effects of hypoxia on metabolism and growth of turtle embryos. *Resp. Physiol.* **92**, 127-138.
Lynn, W. G. and Von Brand, T. (1945). Studies on the oxygen consumption and water metabolism of turtle embryos. *Biol. Bull.* **88**, 112-125.
McGlashan, J. K., Loudon, F. K., Thompson, M. B. and Spencer, R.-J. (2015). Hatching behavior of eastern long-necked turtles (*Chelodina longicollis*): the influence of asynchronous environments on embryonic heart rate and phenotype. *Comp. Biochem. Physiol.* **188A**, 58-64.
Miller, K. and Packard, G. C. (1992). The influence of substrate water potential during incubation on the metabolism of embryonic snapping turtles (*Chelydra serpentina*). *Physiol. Zool.* **65**, 172-187.
Mulder, T. L. M., Golde, J. C., Prinzen, F. W. and Blanco, C. E. (1997). Cardiac output distribution in the chick embryo from stage 36 to 45. *Cardiovasc. Res.* **34**, 525-528.

Nechaeva, M. V., Vladimirova, I. G. and Alekseeva, T. A. (2007). Oxygen consumption as related to the development of the extraembryonic membranes and cardiovascular system in the European pond turtle (*Emys orbicularis*) embryogenesis. *Comp. Biochem. Physiol. A Mol. Integr. Physiol.* **148**, 599-610.
Piiper, J., Tazawa, H., Ar, A. and Rahn, H. (1980). Analysis of chorioallantoic gas exchange in the chick embryo. *Resp. Physiol.* **39**, 273-284.
Reid, K. A., Margaritoulis, D. and Speakman, J. R. (2009). Incubation temperature and energy expenditure during development in loggerhead sea turtle embryos. *J. Exp. Mar. Biol. Ecol.* **378**, 62-68.
Sartori, M. R., Leite, C. A. C., Abe, A. S., Crossley, D. A. and Taylor, E. W. (2015). The progressive onset of cholinergic and adrenergic control of heart rate during development in the green iguana, *Iguana iguana*. *Comp. Biochem. Physiol. A Mol. Integr. Physiol.* **188**, 1-8.
Sartori, M. R., Abe, A. S., Crossley, D. A. and Taylor, E. W. (2017). Rates of oxygen uptake increase independently of changes in heart rate in late stages of development and at hatching in the green iguana, *Iguana iguana*. *Comp. Biochem. Physiol. A Mol. Integr. Physiol.* **205**, 28-34.
Spencer, R.-J., Thompson, M. B. and Banks, P. B. (2001). Hatch or wait? A dilemma in reptilian incubation. *Oikos* **93**, 401-406.
Stecyk, J. A. W., Overgaard, J., Farrell, A. P. and Wang, T. (2004). α-Adrenergic regulation of systemic peripheral resistance and blood flow distribution in the turtle *Trachemys scripta* during anoxic submergence at 5°C and 21°C. *J. Exp. Biol.* **207**, 269-283.
Stewart, J. R. and Florian, J. D. (2000). Ontogeny of the extraembryonic membranes of the oviparous lizard, *Eumeces fasciatus* (Squamata: Scincidae). *J. Morphol.* **244**, 81-107.
Taylor, E. W., Leite, C. A. C., Sartori, M. R., Wang, T., Abe, A. S. and Crossley, D. A., II. (2014). The phylogeny and ontogeny of autonomic control of the heart and cardiorespiratory interactions in vertebrates. *J. Exp. Biol.* **217**, 690-703.
Tazawa, H. and Mochizuki, M. (1977). Oxygen analyses of chicken embryo blood. *Resp. Physiol.* **31**, 203-215.
Thompson, M. B. (1989). Patterns of metabolism in embryonic reptiles. *Resp. Physiol.* **76**, 243-255.
Thompson, M. B. (1993). Oxygen consumption and energetics of development in eggs of the leatherback turtle, *Dermochelys coriacea*. *Comp. Biochem. Physiol. A Physiol.* **104**, 449-453.
Thompson, M. B. and Russel, K. J. (1998). Metabolic cost of development in one of the world's smallest lizard eggs: implications for physiological advantages of the amniote egg. *Copeia.* **1998**, 1016-1020.
Thompson, M. B. and Russel, K. J. (1999). Embryonic energetics in eggs of two species of australian skink, *Morethia boulengeri* and *Morethia adelaidensis*. *J. Herpetol.* **33**, 291-297.
Thompson, M. B. and Stewart, J. R. (1997). Embryonic metabolism and growth in lizards of the genus Eumeces. *Comp. Biochem. Physiol. A Physiol.* **118**, 647-654.
Tucker, V. A. (1967). Method for oxygen content and dissociation curves on microliter blood samples. *J. appl. Physiol.* **23**, 410-414.
Vleck, C. M. and Hoyt, D. F. (1991). Metabolism and energetics of reptilian and avian embryos. In *Egg Incubation: Its Effects in Embryonic Development in Birds and Reptiles* (ed. D. C. Deeming and M. W. J. Ferguson), pp. 285-306. Cambridge: Cambridge University Press.
Warburton, S. J., Hastings, D. and Wang, T. (1995). Responses to chronic hypoxia in embryonic alligators. *J. Exp. Biol.* **273**, 44-50.
Webb, G. J. W., Manolis, S. C., Whitehead, P. J. and Dempsey, K. (1987). The possible relationship between embryo orientation opaque banding and the dehydration of albumen in crocodile eggs. *Copeia* **1987**, 252-257.
Whitehead, P. J. and Seymour, R. S. (1990). Patterns of metabolic rate in embryonic crocodilians *Crocodylus johnstoni* and *Crocodylus porosus*. *Physiol. Zool.* **63**, 334-352.
Yntema, C. L. (1968). A series of stages in the embryonic development of *Chelydra serpentina*. *J. Morphol.* **125**, 219-252.